Bubble size distributions in a convecting layer

Atsuko Namiki,[1] Tadahiro Hatakeyama,[2] Atsushi Toramaru,[1] Kei Kurita,[3] and Ikuro Sumita[1]

[1] We have conducted a series of laboratory experiments to explore the bubble size distribution coupled with convection in a magma chamber. Boiling liquid heated from below exhibits two types of convection pattern depending on the viscosity. When the viscosity is sufficiently high, bubbles are distributed uniformly in the liquid, and the bubble size distribution becomes the power law type for large bubbles and exponential distribution for small bubbles. On the other hand, when the viscosity is low, bubbles are separated from the liquid layer, making a foam, and their size distribution is exponential for large bubbles and unimodal for small bubbles. These experimental results suggest that the bubble size distribution is determined whether the viscous drag of the magma is sufficiently high to trap bubbles. *INDEX TERMS:* 3220 Mathematical Geophysics: Nonlinear dynamics; 8429 Volcanology: Lava rheology and morphology; 8439 Volcanology: Physics and chemistry of magma bodies. **Citation:** Namiki, A., T. Hatakeyama, A. Toramaru, K. Kurita, and I. Sumita, Bubble size distributions in a convecting layer, *Geophys. Res. Lett.*, *30*(15), 1784, doi:10.1029/2003GL017156, 2003.

1. Introduction

[2] Bubble size distribution (BSD) in volcanic clasts has been investigated to deduce the eruption processes in the magma chamber and the conduit (e.g., *Mangan et al.* [1993]). Unimodal, exponential, and power law (fractal) distributions have been reported as typical ones (e.g., *Toramaru* [1990], *Mangan et al.* [1993], *Gaonac'h et al.* [1996b]). Unimodal distribution has been explained by a single event of bubble nucleation and growth by a decompression (*Toramaru* [1989], *Blower et al.* [2001]). Exponential distribution has been interpreted as a result of continuous bubble nucleation and growth (*Marsh* [1988]). Although these two types are explained by simple models, the origin of the power law distribution is not clearly understood. *Blower et al.* [2003] shows that repeated nucleation results in the power law distribution, and *Gaonac'h et al.* [1996a] shows that the power law distribution is a result of coalescence of bubbles. In both cases, the interaction of bubbles would critically affect the BSD and the power law exponent.

[3] As a mechanism for a vesiculation process, the decompression has been mostly considered. However, bubbles also vesiculate by heating and cooling. For example, magma chamber can be heated from below by the ascending magma. Also as the magma chamber cools, crystallization decreases the solubility of volatiles, and the bubbles vesiculate. In addition, under such situation, thermal convection would occur, which in turn would affect the BSD from coalescence caused by shear flow. Although, there are numerous studies on the effect of shear flow on the coalescence of liquid suspensions (e.g., *Burkhart et al.* [2001]), experiments on how the bubbles coalescence under shear flow are rare. In this study, using analogue experiments, we show how the convection driven by basal heating affects the BSD.

2. Experimental Method

[4] We conducted thermally driven degassing experiments using Whole milk and Whip cream as analogues of the magma system. Milk and cream contain water, fat, and protein (Table 1). When milk and cream are boiled, the evaporating water makes bubbles. Proteins whose molecules have long chains stably support the bubble wall; as a result, a vesiculation process similar to that in magma is observed. The lower water content of cream results in a higher viscosity compared to milk. The most significant difference in the physical properties of milk and cream is found in their viscosity. The viscosity of cream is 17 times that of milk. The viscosity of milk/cream without bubbles is measured as a function of temperature ($20-90°C$). The difference in viscosity resulting from temperature variation in this range is a factor of 2.

[5] A cylindrical beaker (130 mm diameter, 300 mm height) is used as the fluid tank and is heated from below at constant heat flux (1.1kW). The volume change, the image of bubbles and convection patterns are recorded using a digital video camera (740 × 480 pixels) and a digital camera (2048 × 1536 pixels). Data on bubble characteristics (number, area A) are obtained from the digitized images using the software "NIH Image". The bubble radius a is calculated by $a = (A/\pi)^{1/2}$. The experiments are conducted under Ca < 1, where $Ca = a\eta_m\dot{\gamma}/\sigma_m$ is the capillary number, η_m is the viscosity of the liquid part, $\dot{\gamma}$ is the shear rate, σ_m is the surface tension. Here, suffix m means the liquid part. σ_m for both of milk and cream is $\sim 50 \pm 10$ mNm^{-1} at 40°C.

3. Results

[6] The experiments show very different features between the two cases. Figure 1 shows time-sequence images of the milk/cream layers. In the case for milk, bubbles separate from the liquid layer and make a foam layer. In the foam region, all bubbles have the same ascending velocity.

---

[1]Department of Earth Sciences, Kanazawa University, Kakuma, Kanazawa, Ishikawa, Japan.
[2]Information Processing Center, Okayama University of Science, Okayama, Japan.
[3]Earthquake Research Institute, Bunkyo, Tokyo, Japan.

Table 1. Physical Properties of the Milk/Cream

Type	Viscosity (mPa·s)	Water (wt%)	Fat (wt%)	protein (wt%)
milk	3	88	3.7	3
cream	50–200[a]	50	47	1.6

[a]We measured the viscosity of the whipped cream with bubbles, which can be considered to be an upper limit estimate for cream.

At a given height, the bubble sizes are uniform. From degassing, the liquid layer decreases with time. After the disappearance of the liquid layer, the foam layer rapidly expands. On the other hand, in the case for cream, most bubbles do not separate from the liquid. The cream convects with bubbles which have a wide range of size distribution.

[7] Figure 2 shows the quantitative relation between the volumetric expansion and the bubble radius. For milk, we find that the average bubble size does not change with time until the liquid layer vanishes, although the volume of the whole layer (liquid + foam) increases as a function of the elapsed time. This indicates that the volumetric increase is caused by the increase of the number of the bubbles. When the liquid layer disappears, the volume increases due to larger average bubbles size. For cream, the temporal variation of the total volume and the bubble radius are approximately synchronous. This indicates that the volumetric increase of the convecting layer is due to the increase of the bubble radius.

[8] The detailed BSDs of these two cases are shown in Figure 3. A snapshot of bubbles in milk foam (Figure 3a) shows the uniformity of bubble size. The measured BSD for milk foam is exponential distribution for large bubbles (>1 mm) and unimodal (Poisson) distribution for small bubbles (<1 mm) (Figure 3b). In contrast, for cream, Figure 3c shows that there is a wide range of bubble size distribution. The measured BSD shows a power law distribution for bubble size larger than 1 mm, and exponential for bubble size less than 1 mm (Figure 3d). Figure 2c shows that there is a relation between the power law exponent and the volumetric change of the convecting layer. When the convecting layer begins to shrink (after 17 min.), the power law exponent becomes larger. We also note that there is spatial variation of the bubble size due to convection. The larger bubbles are concentrated in the upwelling region, whereas the smaller bubbles are observed at the top of the convecting layer and at the downwellings (Figure 1b).

4. Discussion

[9] The experimental results show that the convection pattern, the spatial distribution of bubbles, and the bubble size distributions are strikingly different between the two cases. For milk, the bubbles separate from the liquid, and make a foam layer. In the foam layer, bubbles are nearly uniform in size. However, for cream, bubbles are trapped in the liquid, and their sizes vary. These results indicate that the convection pattern and the BSD depend on whether there is separation of bubbles from the liquid. If the buoyancy force acting on the bubble is large, the bubble will ascend and float above the liquid layer. On the other hand, if the viscous drag arising from the convection is large, the bubble will remain suspended in the liquid. Thus, we infer that the separation of the bubbles from the liquid is determined by the relative magnitude of buoyancy force

F_b and viscous drag F_v. This idea is similar to that of the crystal settling in a convecting layer (*Martin and Nokes* [1988], *Solomatov and Stevenson* [1993]).

[10] The buoyancy force acting on a bubble can be scaled as, $F_b \sim \Delta\rho g a^3$, where $\Delta\rho$ is the density difference between liquid and vapor, and g is the gravitational acceleration. The viscous drag acting on the bubble can be scaled as, $F_v \sim \eta_m v_m a$, where v_m is the convecting velocity. When the convection is vigorous, the convecting velocity v_m is estimated by the Stokes velocity, whose radius is a thickness of a thermal boundary layer of the convection,

$$v_m \sim \frac{\rho_m g \alpha_m \Delta T \delta_{th}^2}{3\eta_m}, \tag{1}$$

where ρ_m is the density of the liquid part, α_m is the thermal expansion coefficient, ΔT is the temperature difference across the convecting layer, $\delta_{th} \sim L/2\xi Ra^\beta$ is the thickness of the thermal boundary layer. L is the thickness of the convecting layer, ξ and β are the experimentally determined constants, Ra is the Rayleigh number for the convecting liquid layer defined as $Ra = \rho_m g \alpha_m \Delta T L^3 / \kappa_m \eta_m$, where κ_m is the thermal diffusivity. Thus, the ratio of F_b to F_v is written as

$$\frac{F_b}{F_v} \sim \frac{\Delta\rho g a^2}{\eta_m v_m} \sim \frac{12\xi^2 \Delta\rho g^{2\beta}}{(\rho_m \alpha_m \Delta T)^{1-2\beta} L^{2-6\beta} \kappa_m^{2\beta}} \frac{a^2}{\eta_m^{2\beta}}. \tag{2}$$

Figure 4a shows the estimated force ratio for bubbles in experiments as a function of viscosity with variable radii of bubbles. In the case for milk (viscosity =3 mPa·s), bubbles with radius larger than 0.1 mm can ascend across the liquid layer. However, the viscosity of cream is 50 mPa·s, which is sufficient to trap small bubbles of the order of 0.1mm. Here, it is known that the viscosity of the bubble bearing suspension increases as a function of the volume fraction of the bubbles when Ca < 0.7 (*Rust and Manga* [2002], *Pal* [2003]). Once the cream layer traps bubbles, the effective viscosity of this layer increases. If the viscosity of the boiling cream is the same as whipped cream, it will reach of the order of 0.1 Pa·s.
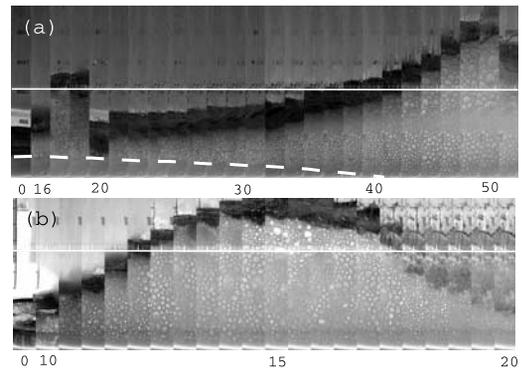
Figure 1. A time-sequence images of the volume and bubble size distribution in a milk and cream, boiled from below. Numbers indicate the elapsed time in minutes. Thin white line indicates the height of 0.1 m. (a) Case for milk: the white broken line shows the boundary between the liquid and the foam layers. The width of the each column is 20 mm. (b) Case for cream: the width of the each column is 25 mm.
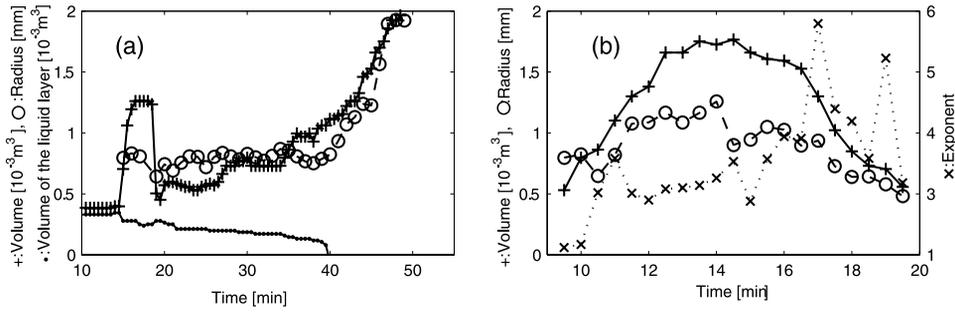
Figure 2. The time evolution of the volume of the whole layer and bubble radius. + is the volume of the layer, ○ is the radius of bubble, and ● is the volume of the remaining liquid layer. × shows the exponent when the BSD is fitted by the power law (see the caption for Figure 3). (a) Case for milk, (b) case for cream.

In addition, the suspending bubbles decrease the mean density of the cream layer, reducing the positive buoyancy of ascending bubbles. Thus, the cream layer can trap larger bubbles. This feedback effect makes the results of milk and cream drastically different, although the viscosity of cream is only 17 times that of milk in the initial condition.

[11] The next question is why the BSDs differ whether the bubbles are trapped in the liquid. When milk is used, the BSD for the foam layer is unimodal for small bubbles (<1 mm) and exponential for large bubbles (>1 mm). If the nucleation of bubbles is instantaneous, and the bubbles reach the top layer at once, then the bubble radii at the top of the liquid layer should be uniform, since the bubbles which nucleate instantaneously are uniform in size (*Toramaru* [1989]). Here, if the next bubble accumulate before the radius of the former bubble changes, the foam layer would

comprise of bubble of the same size. In a foam layer made of uniform bubbles size, coalescence would be inefficient. This is because for coalescence to occur, a pressure gradient between the adjacent bubbles is needed, which result from the difference in bubbles size. Actually, we did not observe any effective coalescence. Thus a foam layer with uniform bubble size forms. The measured BSD for large bubbles is exponential distribution, which can be attributed to the difference in elapsed time after bubble nucleation.

[12] When cream is used, the BSD is exponential for small bubbles (<1 mm) and power law for large bubbles (>1 mm). This can be attributed to the bubble-bearing convection. A turbulence in the flow would cause collision between bubbles, and result in bubble coalescence, since both upwelling and downwelling regions contain bubbles. Once horizontal variation of the bubble size is established, large bubbles ascend faster than surrounding bubbles. Large bubbles rise faster than small bubbles and absorb the small bubbles as they rise. This also causes the bubble size variation. Thus, the BSD for large bubbles which have coalesced become power law distribution. Here, the measured BSD for small bubbles has exponential distribution. This suggests that the BSDs for small bubbles does not appear to have coalescence and have formed through continuous nucleation and growth. Experiments also indicate that the power law exponent for large bubbles change
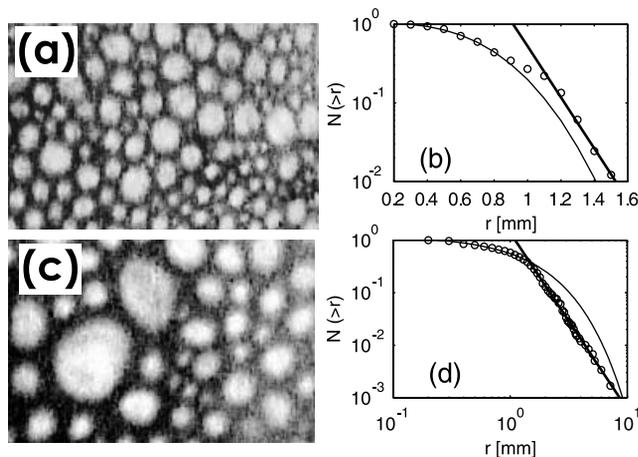
Figure 3. (a) A typical structure of a milk foam, 36 minutes after the beginning of heating. The size of the image is 3×2 cm. (b) the BSD for (a). N is the cumulative number density. ○ shows the measured BSD. Thin line shows the unimodal distribution, $N(>r) \propto \exp(-\lambda r^3)$, where $\lambda = 7.5$. and thick line shows the exponential distribution, $N(>r) \propto \exp(-\lambda r)$, where $\lambda = 1.7$. X-axis is plotted in a linear scale. (c)(d) Same as (a)(b), but for cream. 14 minutes after the beginning of heating. Thick line shows the power law distribution, $N(>r) \propto r^{-d}$, where, the power law exponent d is 3.4. Thin line shows the exponential distribution, $N(>r) \propto \exp(-\lambda r)$, where $\lambda = 0.77$. X-axis is plotted in a log scale.
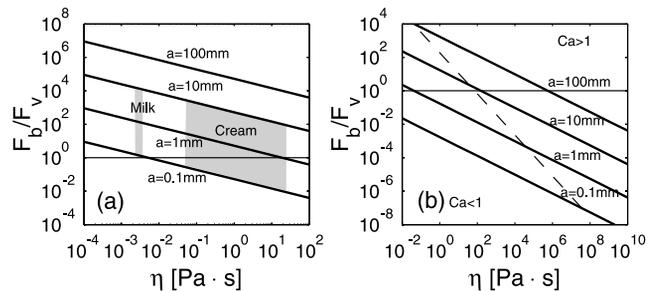
Figure 4. (a) Estimated ratio of the buoyancy force to the viscous drag for the experiments. Here, we used $\Delta \rho = 1000$ kg m^{-3}, g = 10 m s^{-2}, $\rho_m = 1000$ kg m^{-3}, $\alpha_m = 2 \times 10^{-4}$ K^{-1}, $\Delta T = 100$ K, $L = 0.05$m, $\kappa_m = 1.5 \times 10^{-7}$ m^2 s^{-1}, $\xi = 0.16$, and $\beta = 0.28$. (b) Same as (a), but for a magma chamber. Here we assumed $\Delta \rho = 2200$ kg m^{-3}, $\rho_m = 2200$ kg m^{-3}, $\alpha_m = 10^{-5}$ K^{-1}, $\Delta T = 1000$K, $L = 1000$ m, and $\kappa_m = 1 \times 10^{-6}$ m^2 s^{-1}. Dashed line shows Ca = 1, where we assumed $\sigma = 0.01$N m^{-1}, and $\dot{\gamma} = v_m/\delta_{th}$.

with time. When the convecting layer is shrinking (after 17 min.), the power law exponent for large bubbles increases, indicating that the exponent depends on the amount of water. At this stage, most of the water has evaporated, resulting in lesser nucleation. Only bubbles that are too small to escape from the convection remain. This results in uniform bubble size, and large exponent.

[13] For the cases for both milk and cream, the BSDs for small bubbles differ from that of the large bubbles, suggesting that the physical process controlling their size are different. The presence of two different scaling regimes has been reported in the actual basaltic lava flow (*Gaonac'h et al.* [1996b]), suggesting the importance to classify the BSD to understand the vesiculation process in magmatic systems.

[14] Finally, we apply this result to magmatic system. In actual volcanic system, bubble formation is caused by combination of heating/cooling and decompression. In our experiments bubbles formed from basal heating, which is one end-member case of the bubble vesiculation. The estimated volumetric fraction of newly nucleated bubbles formed from heating in a magma chamber is 5 times those of our experiments (see appendix for details). Thus the normalized heat fluxes in our experiments are approximately comparable to that of the magma chamber, and we can apply our results to the processes occuring there.

[15] We can obtain the condition for bubble separation in convecting magma, and can discuss how this is related to BSD. In (Figure 4b), we show the force balance in magmatic system, together with region Ca < 1, since our experiment was for Ca < 1 and BSD might depend on Ca (*Burkhart et al.* [2001]). From this figure, we find that the separation of bubbles from the convecting magma can only occur for magma with very low viscosity (<10 Pa·s) and with large bubbles (>1 mm). This means that in a vigorously convecting magma chamber, most bubbles are trapped in the convecting magma. The bubbles collide with each other and the BSD would become power law for large bubbles and exponential for small bubbles. It follows that we can interpret the unimodal/exponential BSD in magmatic system to have not formed from heating/cooling process.

Appendix A: Volume Fraction of Bubbles

[16] It is known that the critical bubble radius vesiculating at the base from heating is about 1/2 the thickness of the thermal boundary layer $a_c \sim \delta_{th}/2$ (*Nishikawa and Fujita* [1982]). Heat transfer by the convection can be expressed as $q_{conv} \sim \kappa_m C_{p\,m} \rho_m \Delta T / \delta_{th}$, where $C_{p\,m}$ is the specific heat. It follows that the nucleation rate per unit area N_a can be expressed as

$$N_a \sim \frac{q_{conv}}{4/3 \pi a_c^3 \rho_b H} \sim \frac{1}{\pi}\left(\frac{1}{\delta_{th}}\right)^4 \frac{\rho_m \kappa_m \Delta T C_{p_m}}{\rho_b H}, \qquad (A1)$$

where H is the latent heat, and ρ_b is the density of the bubble. If the nucleated bubbles ascend at Stokes velocity $v_b \sim \Delta\rho g a_c^2/3\eta_m$, the number of the distributing bubbls per unit volume is $N_v \sim N_a/v_b$. Neglecting the growth of bubbles and assuming $\beta \sim 1/3$ to simplify the scaling, we

obtain the expression for volume fraction of dispersed bubbles ϕ,

$$\phi \sim N_v \cdot \frac{4}{3}\pi a_c^3 \sim \frac{\rho_m^2 \alpha_m \Delta T^2 C_{p_m}}{\rho_b \Delta\rho H}. \qquad (A2)$$

Note that this expression does not depend on the magma viscosity and the depth of the convecting layer. In the experiments $\Delta\rho = 1000$ kg m^{-3}, $\rho_m = 1000$ kg m^{-3}, $\rho_b = 0.5$ kg m^{-3}, $\alpha_m = 2 \times 10^{-4}$ K^{-1}, $\Delta T = 100$ K, $C_{p\,m} = 4200$ J kg^{-1}, $H = 2.2 \times 10^6$ J kg^{-1}. In the magma chamber the plausible values are, $\Delta\rho \sim 2200$ kg m^{-3}, $\rho_m \sim 2200$ kg m^{-3}, $\rho_b \sim 0.5$ kg m^{-3}, $\alpha_m \sim 10^{-5}$ K^{-1}, $\Delta T \sim 1000°$K, $C_{p\,m} \sim 900$ J kg^{-1}. $H \sim 10^6$ J kg^{-1} (*Sahagian and Proussevitch* [1996]). Using these values, we find that ϕ for magmatic system is 5 times of that of the experiments.

References

Blower, J. D., J. P. Keating, H. M. Mader, and J. C. Phillips, Inferring volcanic degassing processes from vesicle size distributions, *Geophys. Res. Lett.*, *28*, 347–350, 2001.

Blower, J. D., J. P. Keating, H. M. Mader, and J. C. Phillips, The evolution of bubble size distributions in volcanic eruptions, *J. Volcanol. Geotherm. Res.*, *120*, 1–23, 2003.

Burkhart, B. E., P. V. Gopalkrishnan, S. D. Hudson, A. M. Jamieson, M. A. Rother, and R. H. Davis, Droplet growth by coalescence in binary fluid mixtures, *Phys. Rev. Lett.*, *87*, 098,304, 2001.

Gaonac'h, H., S. Lovejoy, J. Stix, and D. Scherzter, A scaling growth model for bubbles in basaltic lava flows, *Earth Planet. Sci. Lett.*, *139*, 395–409, 1996a.

Gaonac'h, H., J. Stix, and S. Lovejoy, Scaling effects on vesicle shape, size and heterogeneity of lavas from Mount Etna, *J. Volcanol. Geotherm. Res.*, *74*, 131–153, 1996b.

Mangan, M. T., K. V. Cashman, and S. Newman, Vesiculation of basaltic magma during eruption, *Geology*, *21*, 157–160, 1993.

Marsh, B. D., Crystal size distribution (csd) in rocks and the kinetics and dynamics of crystallization.1. theory, *Contrib. Mineral. Petrol.*, *99*, 277–291, 1988.

Martin, D., and R. Nokes, Crystal settling in a vigorously convecting magma chamber, *Nature*, *332*, 534–536, 1988.

Nishikawa, K., and Y. Fujita, *Heat Transfer (in Japanese "Dennetsu Gaku")*, RikohGaku-sha, 1982.

Pal, R., Rheological behavior of bubble-bearing magmas, *Earth Planet. Sci. Lett.*, *207*, 165–179, 2003.

Rust, A. C., and M. Manga, Effects of bubble deformation on the viscosity of dilute suspensions, *J. Non-Newtonian Fluid Mech.*, *104*, 53–63, 2002.

Sahagian, D. L., and A. A. Proussevitch, Thermal effects of magma degassing, *J. Volcanol. Geotherm.*, *74*, 1996.

Solomatov, V. S., and D. J. Stevenson, Suspension in convective layers and style of differentiation of a terrestrial magma ocean, *J. Geophys. Res.*, *98*, 5375–5390, 1993.

Toramaru, A., Vesiculation process and bubble-size distributions in ascending magmas with constant velocities, *J. Geophys. Res.*, *94*, 17,523–17,542, 1989.

Toramaru, A., Measurement of bubble-size distributions in vesiculated rocks with implications for quantitative estimation of eruption processes, *J. Volcanol. Geotherm. Res.*, *43*, 71–90, 1990.

———————————
A. Namiki, A. Toramaru, and I. Sumita, Department of Earth Sciences, Kanazawa University, Kakuma, Kanazawa, Ishikawa 920-1192, Japan. (namiki@earth.s.kanazawa-u.ac.jp)

T. Hatakeyama, Information Processing Center, Okayama University of Science, 1-1, Ridai-cho Okayama 700-0005, Japan.

K. Kurita, Earthquake Research Institute, 1-1-1, Yayoi, Bunkyo, Tokyo 113-0032, Japan.